ELSEVIER

Journal of Alloys and Compounds 446–447 (2007) 44–47

Journal of ALLOYS AND COMPOUNDS

www.elsevier.com/locate/jallcom

A new series of high hydrogen content hydrogen-storage materials—A theoretical prediction

P. Vajeeston*, P. Ravindran, H. Fjellvåg

Center for Materials Sciences and Nanotechnology, Department of Chemistry, University of Oslo, Box 1033 Blindern, N-0315 Oslo, Norway

Received 24 October 2006; received in revised form 8 December 2006; accepted 13 December 2006
Available online 21 December 2006

Abstract

The structural phase stability of $NaBeH_3$, $NaMgH_3$, and $Ca(BH_4)_2$ has been investigated using density-functional projector-augmented-wave method within the generalized-gradient approximation. Among the various structural arrangements used as inputs for the structural optimization calculations, the experimentally known frameworks are successfully reproduced for $NaMgH_3$ and the positional and unit-cell parameters are found to be in good agreement with the experimental finding. The crystal structure of $NaBeH_3$ and $Ca(BH_4)_2$ has been predicted. The electronic density of states reveal that all the considered compounds are wide-band-gap insulators.

Keywords: Crystal structure of $NaBeH_3$ and $Ca(BH_4)_2$; Hydrogen storage materials; Alkali and alkaline-earth based hydrides

1. Introduction

The implementation of the “hydrogen economy" demands access to materials with a high weight-percentage of hydrogen which can operate (hydrogen loading/unloading) at acceptable temperatures and costs. Up-to-date known hydrides (metal as well as complex hydrides) are unable to fulfil these requirements. Several complex hydrides have high hydrogen content, but unfortunately poor kinetics and lacking reversibility with respect to hydrogen absorption/desorption. Recent experimental findings have shown that the decomposition temperature for certain complex hydrides can be modified by introduction of additives [1,2]. This has opened up for research activity on identification of appropriate admixtures for known or hitherto unexplored complex hydrides.

The crystal structures of the pure elements and most of the binary compounds have been frequently studied and are well characterized. On turning to ternary compounds, however, the amount of knowledge is considerably less extensive (with an estimated 10% coverage of structural information), and for quaternary and multi-component phases the structural knowledge is extremely poor. For hydrides, owing to the complexity in structural arrangements and difficulties involved in establishing hydrogen positions by X-ray diffraction methods, structural informations are very limited [3]. As proposed in our earlier communications, it should be possible to form several series of hydrides with alkali and alkaline-earth metals in combination with group III elements of the periodic table, but only few members of these series have so far been experimentally explored. At present we focus on new materials like $MM'H_3$ (M = alkali and M′ = alkaline-earth element, e.g., $LiBeH_3$, $NaMgH_3$, etc.), $M'AH_5$ (A = group III elements, e.g., $MgAlH_5$, $BaAlH_5$, etc. [4]) and $M'(BH_4)_2$. Mg-based hydrides have received special attention because of their lower weight and manufacturing costs. In particular, $Mg(AlH_4)_2$ has been in the focus of interest because, out of the theoretical 9.3 wt.% hydrogen, 7 wt.% may be extracted at temperatures as low as 135–163 °C [5–7]. However, the lack of reversibility represents a yet unsolved problem. In analogy with $Mg(AlH_4)_2$ it is possible to imagine a series of compounds with the general formula $M(BH_4)_2$ (M = Be, Mg, Ca, Sr, Ba). $Mg(BH_4)_2$ can theoretically store up to 16.8 wt.% H and its existence and synthesis route are already indicated in the literature [8]. In this article we are demonstrating the predicting capability of theory for some high hydrogen content known $NaMgH_3$, and unknown $NaBeH_3$ and $Ca(BH_4)_2$ phases. In addition to the crystal structure exploration, electronic structure and associated properties of these phases are also investigated within the scope of density-functional theory.

* Corresponding author.
E-mail address: ponniahv@kjemi.uio.no (P. Vajeeston).

0925-8388/$ – see front matter © 2006 Elsevier B.V. All rights reserved.
doi:10.1016/j.jallcom.2006.12.058

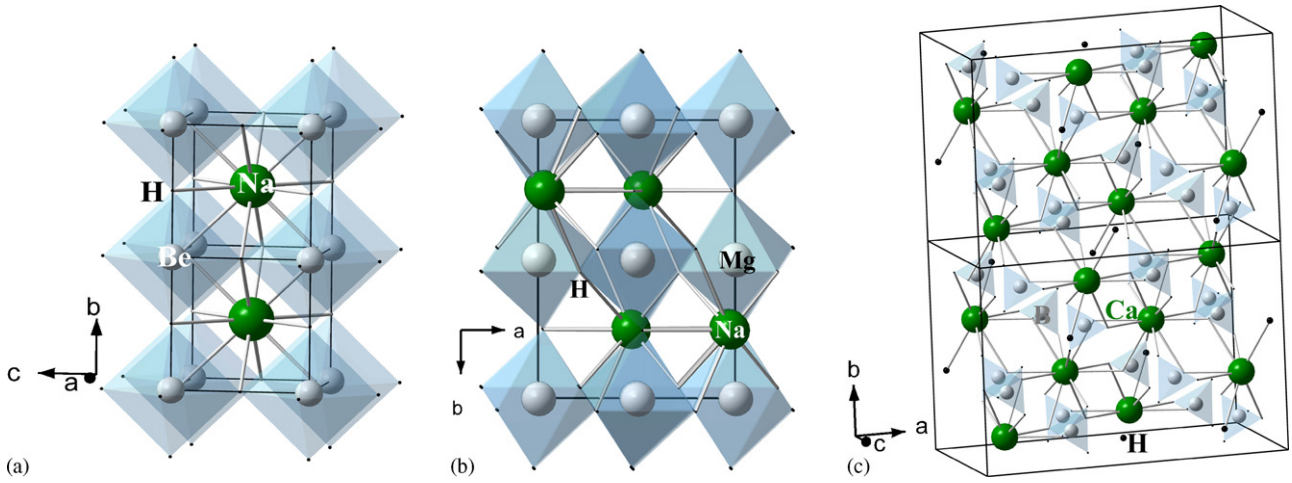

Fig. 1. Optimized ground-state crystal structure for (a) $NaBeH_3$ ($CaTiO_3$ type, ideal perovskite; $Pm\bar{3}m$); (b) $NaMgH_3$ ($GdFeO_3$ type, deformed perovskite; *Pnma*); (c) α-$Ca(BH_4)_2$.

Total energies have been calculated using the projected–augmented plane-wave (PAW) [9] implementation of the Vienna *ab initio* simulation package (VASP) [10]. The generalized-gradient approximation (GGA) [11] was used to obtain accurate exchange and correlation energies for particular configurations of atoms. Ground-state geometries were determined by minimizing stresses and Hellman–Feynman forces with the conjugate-gradient algorithm, until forces on all atomic sites were less than 10^{-3} eV Å^{-1}. Brillouin zone integration was performed with a Gaussian broadening of 0.1 eV during all relaxations. In order to span a wide range of energetically accessible crystal structures, unit-cell volume and shape as well as atomic positions were relaxed simultaneously using a series of calculations with progressively increasing precision. A final high accuracy calculation of the total energy was performed after completion of the relaxations with respect to **k**-point convergence and plane-wave cutoff. From various sets of calculations it was found that 512 **k** points in the whole Brillouin zone with a 500 eV plane-wave cutoff are sufficient for the $NaMgH_3$ structure to ensure optimum accuracy in the computed results. A similar density of **k** points and energy cutoff were used for the other structures/phases considered. The present type of theoretical approach has recently been applied to explore ambient- and high-pressure phases of hydrogen storage materials, which in many cases have later been experimentally verified.

1.1. Structural features of $NaBeH_3$ and $NaMgH_3$

Following 24 potentially applicable structure types have been used as inputs in the structural optimization calculations for the $MMgH_3$ compounds (Pearson structure classification notation in parenthesis): $KMnF_3$ (*tP*20), $GdFeO_3$ [$NaCoF_3$ (*oP*20)], $KCuF_3$ (*tI*20), $BaTiO_3$ [$RbNiF_3$ (*hP*30)], $CsCoF_3$ (*hR*45), $CaTiO_3$ [$CsHgF_3$ (*cP*5)], PCF_3 (*tP*40), $KCuF_3$ (*tP*5), $KCaF_3$ (*mP*40), $NaCuF_3$ (*aP*20), $SnTlF_3$ (*mC*80), $KCaF_3$ (*mB*40), $LiTaO_3$ (*hR*30), $KCuF_3$ (*oP*40), $CaCO_3$ (*mP*20), $KNbO_3$ (*tP*5), $KNbO_3$ (*oA*10), $KNbO_3$ (*hR*5), $LaNiO_3$ (*hR*30), $CaTiO_3$ (*oC*10), $FeTiO_3$ (*hR*30), $SrZrO_3$ (*oC*40), $BaRuO_3$ (*hR*45), and α-$CsMgH_3$ (*Pmmm*) [12,13]. From the above structural starting points, full geometry optimization has been carried out without any constrains on the atomic positions and unit-cell parameters. It should be noted that, during the structural relaxation, some of the initial structures are converted into another structure type or a new structure which was not included among the selected guess structures.

The crystal structure of $NaMgH_3$ is already known and this has been considered as a distorted perovskite structure [Fig. 1(b)] analogous to the $GdFeO_3$ type [14–16]. Consistent with the experimental findings, the structural optimizations show that, this atomic arrangement has lower energy than the considered alternatives (see above) and the calculated unit-cell dimensions and positional parameters at 0 K and ambient pressure are in good agreement with the room temperature experimental results (see Table 1). The deviations from the experimental unit-cell parameters *a* and *b* are almost zero and the underestimation of 1.2% in the *c* direction is typical for the state-of-art approximation of density-functional theory. This finding shows that one can reliably reproduce/predict structural parameters for even quite complex atomic arrangements with this type of approach. When we compare the interatomic distances, the Na–H distances are varying over a larger range from 2.302 to 2.701 Å, while, the Mg–H distances are varying from 1.967 to 1.976 Å. These values are consistent with the experimental observation, where the Na–H distances are varying between 2.26 and 2.47 Å and the Mg–H separation varies between 1.957 and 1.979 Å. As seen from Table II, the MgH_6 octahedra in $NaMgH_3$ are somewhat distorted (H–Mg–H angles are in the range of 88.2–91.8°). A similar structure with the same type of distortions is incidently also found for $NaMgF_3$ [16]. In general, most of the hydride and fluoride families show pronounced analogies in structural aspects.

The crystal structure of $NaBeH_3$ is not yet identified experimentally. According to the structural optimization calculations with the considered 24 structural inputs, the $CaTiO_3$ type variant [Table 1, Fig. 1(a)] is found to have the lowest total energy. The $NaBeH_3$ structure consists of corner sharing ideal BeH_6 oc-

Table 1
Optimized equilibrium structural parameters, bulk modulus (B_0), and pressure derivative of bulk modulus (B_0') for $NaBeH_3$, $NaMgH_3$, and $Ca(BH_4)_2$ phases

Compound (structure type; space group)	Unit-cell (Å)	Positional parameters	B_0 (GPa)	B_0'
$NaBeH_3$ ($CaTiO_3$ type; $Pm\bar{3}m$)	$a = 3.2662$	Na (1*b*): 1/2, 1/2, 1/2 Be (1*a*): 0, 0, 0 H (3*d*): 0, 0, 1/2	62.7	3.5
$NaMgH_3$ ($GdFeO_3$ type; *Pnma*)	$a = 5.4525$ (5.4634)[a] $b = 7.6952$ (7.7030)[a] $c = 5.3683$ (5.4108)	Na (4*c*): 0.0209, 1/4, 0.006 Mg (4*b*): 0, 0, 1/2 H1 (4*c*): 0.503, 1/4, 0.093 H2 (8*d*): 0.304, 0.065, 0.761	38.4	3.6
$Ca(BH_4)_2$ ($Ba(MnO_4)_2$ type; *Fddd*)	$a = 13.1491$ $b = 8.8052$ $c = 7.4799$	Ca (8*b*): 1/8, 5/8, 1/8 B (16e): 0.3462, 1/8, 5/8 H1 (32*h*): 0.2931, 0.1250, 0.7607 H2 (32*h*): 0.5996, 0.9875, 0.3858	16.6	5.1

[a] Experimental value from Ref. [14].

tahedra [see Fig. 1(a)]. In $NaBeH_3$, Na is surrounded by 12 H in cuboctahedral coordination at a distance of 2.31 Å and Be is octahedrally coordinated to six H at a distance of 1.63 Å, H is surrounded by two Be and four Na, and the shortest H–H separation is 2.31 Å. The crystal structure of both $NaBeH_3$ and $NaMgH_3$ belongs to perovskite family. Generally, the A-site cations in an ideal perovskite structure (ABX_3) are larger than the B-site cations and similar in size to the X-site anions. In relation to $NaBeH_3$ we note that the tabulated ionic radius for Na^+ is larger than that for Be^{2+} and H^-, but the Be^{2+} radius is only around half of the H^- radius [13,17]. This finding appears to emphasize the significance of size factors associated with both cations and anions (in particular H^-) for stabilization of an ideal/inverse perovskite arrangement.

1.2. Structural features of $Ca(BH_4)_2$

Twenty eight potentially applicable structure types have been used as inputs in the structural optimization calculations for the $Ca(BH_4)_2$ phases (used input structural modifications are given in Ref. [18]). The structural optimization calculations for $Ca(BH_4)_2$ phase show that the $Ba(MnO_4)_2$ type input structure has the lowest total energy. It is interesting to note that $Mg(AlH_4)_2$ system consists of slightly distorted MgH_6 octahedron and AlH_4 tetrahedra. These polyhedra are bridged by a hydrogen resulting in a structure with a sheet-like arrangement along the *c* axis [7,19]. On the other hand, in $Ca(BH_4)_2$ the atomic arrangement exhibits three dimensional network (see Fig. 1(d)). The $Ca(BH_4)_2$ structure consists of slightly distorted BH_4 tetrahedra with B–H distances varying between 1.22 and 1.23 Å and the H–B–H bond angle varies from 106 to 113°. All the H atoms in the BH_4 tetrahedra are linked by two nearest neighbor Ca atoms. These Ca atoms are surrounded by eight hydrogen atoms with Ca–H distances varying between 1.992 and 2.208 Å. Application of high-pressure transforms this structure type to a few other high-pressure structural modifications. The high-pressure behavior of these studied phases along with other compounds in the rest of the series will appear in a forthcoming article.

By fitting the total energy as a function of cell volume using the so-called universal equation of state [20], the bulk modulus (B_0) and its pressure derivative (B_0') are obtained (Table 1), but no experimental data are yet available for comparison. Compared to intermetallic-based hydride phases, all these phases have low B_0 values implying that these materials are soft and easily compressible. Hence, one can expect that de-stabilization of some of the hydrogen atoms from the matrix may be feasible. However, the Be–H and/or B–H bonds are likely to be strong. In fact, the experience from other complex aluminium-containing hydrides shows that one needs high temperature to break Al–H bonds (Fig. 2).

The calculated total DOSs for $NaBeH_3$, $NaMgH_3$, and $Mg(BH_4)_2$ in the ground-state configurations are shown in Fig. 3. All the studied compounds have finite energy gaps (from 2.4 to 4.9 eV) between the valence band and the conduction band (CB) and are hence, proper insulators. In $Ca(BH_4)_2$ the valence band is split into two bands. A similar feature is observed [21] for $LiAlH_4$ and $NaAlH_4$. Common structural features for all these phases is the tetrahedral BH_4/AlH_4 units and a very similar

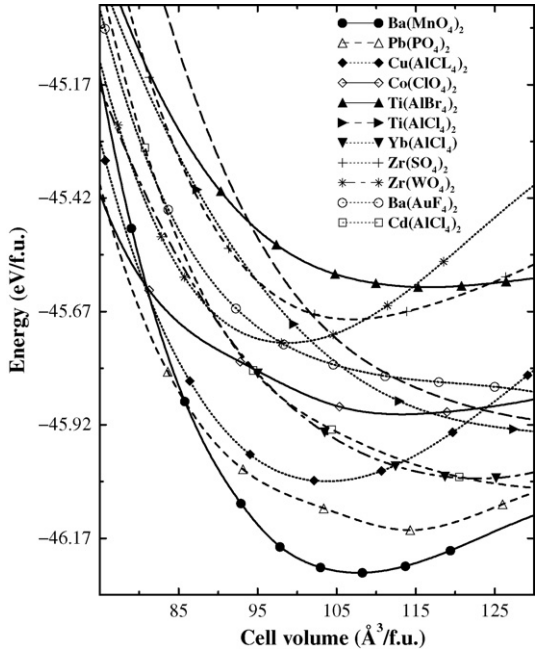

Fig. 2. Calculated unit-cell volume vs. total energy for $Ca(BH_4)_2$ in possible structural arrangements (for the better view only 11 structural modifications are shown.

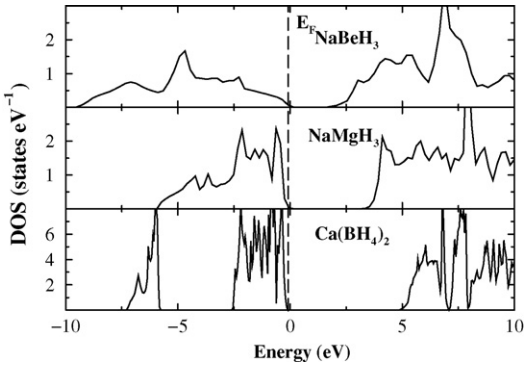

Fig. 3. Calculated total DOSs for $NaMgH_3$, $NaBeH_3$, and $Ca(BH_4)_2$ compounds. The Fermi level is set to zero energy and marked by the vertical dotted line.

bonding situation. The basically ionic interaction between Mg and BH_4/AlH_4 also has its parallel for alkali-metal-to-AlH_4 interaction in $LiAlH_4$ and $NaAlH_4$. More specifically we see the B–H/Al–H interaction within the BH_4/AlH_4 tetrahedra as iono-covalent and that between Mg and H more as pure ionic. On the other hand, in $NaBeH_3$ and $NaMgH_3$ phases the valence band become a single region and the interaction between Be/Mg–H and Na–H has predominant ionic character.

2. Conclusion

The crystal and electronic structures of $NaMgH_3$, $NaBeH_3$, and $Ca(BH_4)_2$ have been studied by state-of-the-art density-functional calculations. The ground-state crystal structures have been identified from structural optimization of a number of structures using force as well as stress minimizations. For the experimentally known compounds, the ground-state structures are successfully reproduced within the accuracy of the density-functional approach. The crystal structures of $NaBeH_3$, and $Ca(BH_4)_2$ have been predicted and one can store up to 11.56 wt.% H in $Ca(BH_4)_2$ phase. The studied compounds are wide-band-gap insulators and the insulating behavior is associated with well-localized, paired s-electron configuration at the H site.

Acknowledgement

The authors gratefully acknowledge the Research Council of Norway for financial support and for computer time at the Norwegian supercomputer facilities.

References

[1] B. Bogdanovic, M. Schwickardi, J Alloys Compd. 253 25 (1997) 1.
[2] B. Bogdanovic, R.A. Brand, A. Marjanovic, M. Schwikardi, J. Tölle, J Alloys Compd. 302 (2000) 36.
[3] K. Yvon, R.B. King (Eds.), Encyclopedia of Inorganic Chemistry, vol. 3, Wiley, NY, 1994.
[4] A. Klaveness, P. Vajeeston, P. Ravindran, H. Fjellvåg, A. Kjekshus, Phys. Rev. B 73 (2006) 094122.
[5] E. Wiberg, R. Bauer, Z. Naturforsch. B 7 (1952) 131.
[6] T.N. Dymova, V.N. Konoplev, A.S. Sizareva, D.P. Aleksandrov, Russ. J. Coord. Chem. 25 (1999) 312.
[7] M. Fichtner, J. Engel, O. Fuhr, A. Gloss, O. Rubner, R. Ahlrich, Inorg. Chem. 356/357 (2003) 178.
[8] H.I. Schlesinger, H.C. Brown, E.K. Hyde, J. Am. Chem. Soc. 75 (1953) 209.
[9] P.E. Blöchl, Phys. Rev. B 50 (1994) 17953;
G. Kresse, J. Joubert, Phys. Rev. B 59 (1999) 1758.
[10] G. Kresse, J. Hafner, Phys. Rev. B 47 (1993) 6726;
G. Kresse, J. Furthmuller, Comput. Mater. Sci. 6 (1996) 15.
[11] J.P. Perdew, in: P. Ziesche, H. Eschrig (Eds.), Electronic Structure of Solids, Akademie Verlag, Berlin, 1991;
J.P. Perdew, K. Burke, Y. Wang, Phys. Rev. B 54 (1996) 16533;
J.P. Perdew, S. Burke, M. Ernzerhof, Phys. Rev. Lett. 77 (1996) 3865.
[12] Inorganic Crystal Structure Database, Gmelin Institut, Germany, 2001, p. 1.
[13] G. Renaudin, B. Bertheville, K. Yvon, J. Alloys Compd. 353 (2003) 175.
[14] A. Bouamrane, J.P. Laval, J.-P. Soulie, J.R. Bastide, Mater. Res. Bull. 35 (2000) 545.
[15] S. Geller, J. Chem. Phys. 24 (1956) 1236.
[16] E. Rönnebro, D. Noréus, K. Kadir, A. Reiser, B. Bogdanovic, J. Alloys Compd. 299 (2000) 101.
[17] R.D. Shannon, Acta Crystallogr. B 32 (1976) 751.
[18] P. Vajeeston, P. Ravindran, H. Fjellvåg, A. Kjekshus, Appl. Phys. Lett. 89 (2006) 071906.
[19] A. Fossdal, H.W. Brinks, M. Fichtner, B.C. Hauback, J. Alloys Compd. 387 (2005) 47.
[20] P. Vinet, J.H. Rose, J. Ferrante, J.R. Smith, J Phys.: Condens. Matter 1 (1989) 1941.
[21] P. Vajeeston, P. Ravindran, R. Vidya, H. Fjellvåg, A. Kjekshus, Cryst. Growth Des. 4 (2004) 471.